Acta Crystallographica Section C
Crystal Structure Communications
ISSN 0108-2701

Clathrate solvates of tetrakis(4-methoxycarbonylphenyl)porphyrin and its zinc(II)–pyridine complex, in which the porphyrin host structures are stabilized by porphyrin–porphyrin stacking and C—H···O attractions

Sankar Muniappan, Sophia Liptsman and Israel Goldberg*

School of Chemistry, Sackler Faculty of Exact Sciences, Tel-Aviv University, Ramat-Aviv, 69978 Tel-Aviv, Israel
Correspondence e-mail: goldberg@post.tau.ac.il

Received 13 February 2006
Accepted 21 February 2006
Online 18 March 2006

Tetrakis(4-methoxycarbonylphenyl)porphyrin, or tetramethyl 4,4′,4″,4‴-porphyrin-5,10,15,20-tetrabenzoate, crystallizes as a nitrobenzene 1.9-solvate, $C_{52}H_{38}N_4O_8\cdot1.9C_6H_5NO_2$, (I). The solvent molecules are contained in extended channels which propagate through the host lattice between parallel screw/glide-related columns of offset-stacked porphyrin entities. Side packing of these columns involves π–π interactions between the methoxycarbonylphenyl residues. Molecules of the porphyrin host lie on crystallographic inversion centres. The zinc(II)–pyridine derivative pyridine(tetramethyl 4,4′,4″,4‴-porphyrin-5,10,15,20-tetrabenzoato)zinc(II), [Zn($C_{52}H_{36}N_4O_8$)(C_5H_5N)], (II), is a square-pyramidal five-coordinate complex with pyridine as an apical ligand, which crystallizes as a chloroform–pyridine solvate. The metalloporphyrin–pyridine units form an open layered arrangement, occluding the non-coordinated solvent moieties within the intralayer interporphyrin voids. Within such arrays, the host porphyrin molecules are in contact with one another through the peripheral methoxycarbonyl substituents. The crystal packing consists of a bilayered arrangement of inversion-related porphyrin layers, with the axial ligands mutually penetrating into the voids of neighbouring arrays and tight offset stacking of these bilayers.

Comment

Tetraarylporphyrins and -metalloporphyrins are extremely versatile host scaffolds for the formation of crystalline inclusion compounds with a large number of guest species (Byrn *et al.*, 1993; Krishna Kumar *et al.*, 1998; Goldberg, 2005). This involves genuine lattice clathrates (without specific bonds between the porphyrin hosts; Byrn *et al.*, 1993), as well as structures wherein functionalized porphyrins are interlinked in two or three dimensions by hydrogen bonding of coordination polymerization (Goldberg, 2005). In this study, we characterize the supramolecular organization of the title compounds, (I) (the free base porphyrin) and (II) (its zinc pyridine complex), which have not been reported before, and describe examples of their clathration behaviour. In relation to the basic tetraphenylporphyrin clathrate host (Byrn *et al.*, 1993), these two compounds have slightly extended arms, bearing an additional methoxycarbonyl group on the *para* positions of the four phenyl substituents, and thus an increased propensity, due to their elongated arms, for the formation of solvates and clathrates (Krishna Kumar *et al.*, 1998). The two structures were analysed at *ca* 110 K.

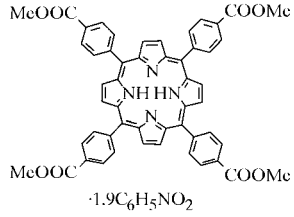

(I)

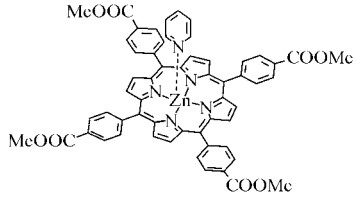

(II)

Compound (I) crystallizes as a nitrobenzene disolvate (Fig. 1), with the porphyrin species located on crystallographic centres of inversion. The macrocyclic core 24-membered ring is planar to within ±0.053 Å, except for atom N21, which deviates by 0.118 (2) Å from this plane. The four aryl substituents are oriented roughly perpendicular to the macrocycle in a typical manner, the dihedral angle between their mean planes and that of the macrocycle being 60.80 (3)° for the C25–C30 group and 69.96 (5)° for the C35–C40 group. Moreover, at every site, the methoxycarbonyl fragments are nearly coplanar with the corresponding aromatic ring to which they are bound, the dihedral angles between their mean planes being only 8.8 (1) and 5.7 (1)°. The two inner pyrrole N-bound H atoms are disordered between the four N-atom sites.

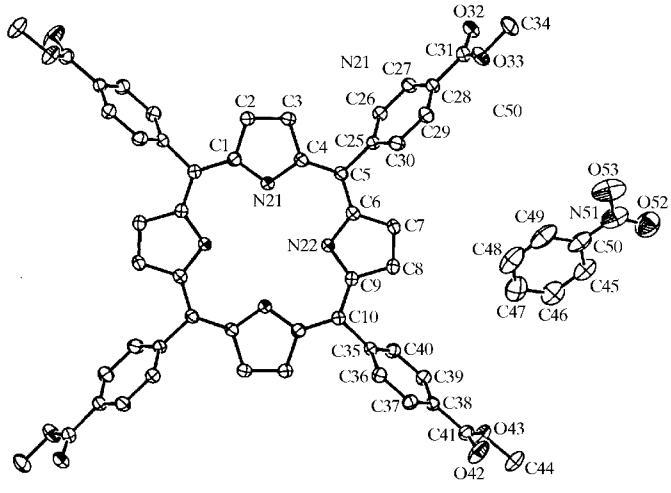

Figure 1
The molecular structure of (I), showing the atom-labelling scheme. Displacement ellipsoids are drawn at the 50% probability level at *ca* 110 K. The porphyrin molecules are located on centres of inversion at ($-x$, $1-y$, $1-z$). H atoms have been omitted.

  DOI: 10.1107/S010827010600641X

The crystal structure of (I) can be best described as consisting of offset-stacked porphyrin columns aligned parallel to the *b* axis of the crystal (Fig. 2). The mean distance between the planes of successive porphyrin macrocycles is 4.15 (5) Å. Sideways, the columns are arranged in an approximate square-grid array. The porphyrin molecules in a given column are tilted by about 45° with respect to the stacking axis (Fig. 3). This intermolecular organization is associated with the presence of channel voids between the porphyrin columns, which are accommodated by the nitrobenzene guest components. The latter are aligned perpendicular to the channel axis, exhibiting antiparallel orientation between successive species in every channel [related by inversion at $(\frac{1}{2} - x, -y - \frac{1}{2}, \frac{1}{2} - z)$]. As shown in Fig. 3, the porphyrin columns are arranged in a herring-bone fashion, and their side packing is characterized by stacking interactions between partly overlapping methoxycarbonylphenyl fragments of adjacent molecules related by the glide/screw symmetry of about 3.7 Å. Some relatively short intermolecular C—H···O contacts, which may represent attractive interactions, are listed in Table 1. These involve host–host contacts within as well as between the porphyrin columns, and a porphyrin–nitrobenzene contact.

The molecular structure of (II) is shown in Fig. 4. Note that the O63–C64 methoxy substituent exhibits orientational disorder. Compound (II) represents a square-pyramidal five-coordinate complex of the porphyrin species, with the inner pyrrole N atoms deviating alternately ±0.021 (1) Å from their mean plane. The central Zn ion is displaced by 0.340 (1) Å from this N_4 plane towards the axial ligand, imparting a domed

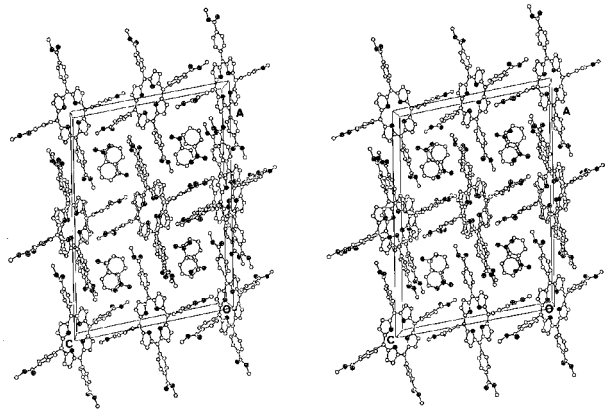

Figure 2
The crystal packing of (I), viewed approximately down the *b* axis. Note the offset-stacked arrangement of the porphyrin molecules that form the host lattice and the antiparallel arrangement of the nitrobenzene solvent incorporated within the channel voids. H atoms have been omitted. N and O atoms are denoted by shaded circles.

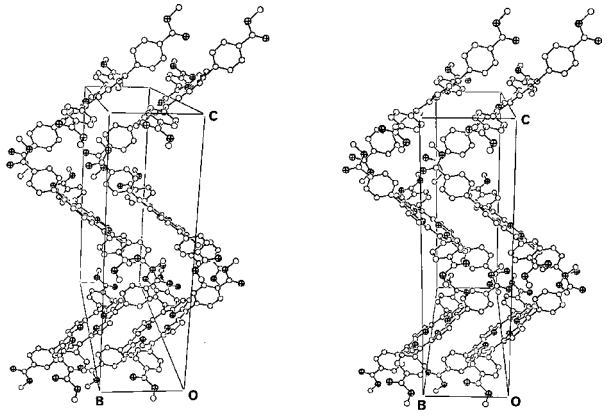

Figure 3
A perspective side view of three neighbouring porphyrin columns of (I) related to one another by the glide/screw symmetry, showing the herring-bone organization and the stacking interaction between the methoxycarbonyl fragments of adjacent columns (see *Comment*). H atoms have been omitted for clarity. N and O atoms are denoted by shaded circles.

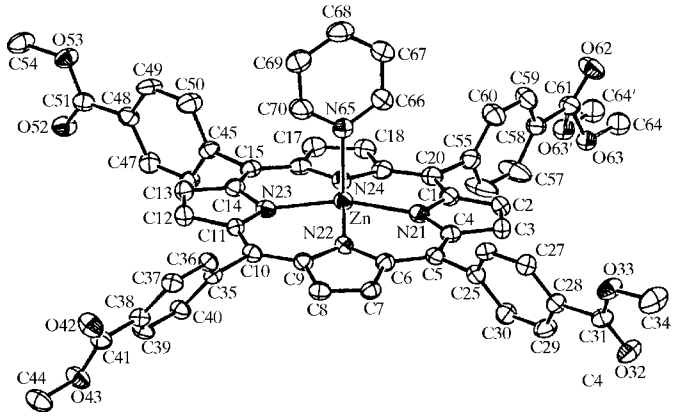

Figure 4
The molecular structure of host (II), showing its domed shape and the atom-labelling scheme. Displacement ellipsoids are drawn at the 40% probability level at *ca* 110 K. Note the orientational disorder of the C61–C64 methoxycarbonyl group (primed atoms).

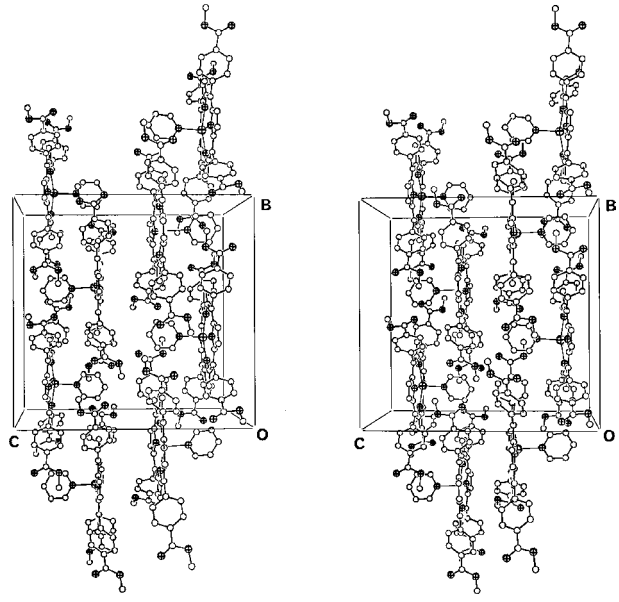

Figure 5
A stereoview of the crystal packing of host molecules in (II) (approximately down *a*), showing their layered organization edge-on and the tight packing of the offset-stacked layers along the *c* axis. Zn, N and O atoms are denoted by shaded circles. H atoms have been omitted.

structure to the metalloporphyrin entity. This is a characteristic of many five-coordinate complexes of metallated tetraarylporphyrins with a single axial ligand [184 hits; Cambridge Structural Database (CSD), Version 5.27, November 2005 update; Allen, 2002; Lipstman *et al.*, 2006; Lipstman & Goldberg, 2006]. Otherwise, the intramolecular conformational features of (II) are similar to those observed in (I). Thus, the dihedral angles between the mean planes of the phenyl substituents and the plane of the four pyrrole N atoms are 67.8 (1), 58.4 (1), 85.4 (1) and 82.1 (1)°, respectively, for the C25–C30, C35–C40, C45–C50 and C55–C60 rings. The mean planes of the corresponding methoxycarbonyl fragments deviate only slightly from coplanarity with their adjacent benzene rings, as indicated by the dihedral angles between the respective phenyl and methoxycarbonyl residues of (in the same order as above) 5.4 (3), 10.2 (3), 7.0 (3) and 7.0 (5)/15.4 (4)°.

The molecules of (II) are arranged in the crystal in a square-layered fashion approximately perpendicular to the *c* axis. Adjacent units in a layer contact one another in all four directions through the peripheral *cis*-related methoxycarbonyl fragments. The corresponding non-bonding contacts between the carbonyl O atoms of one porphyrin to the methyl C atoms are O32···C64($x-1, y, z$) = 3.356 (5) Å and O32···C64′($x-1$, y, z) = 3.141 (6) Å, O42···C44(x, $y-1$, z) = 3.621 (5) Å, O52···C44($x+1$, y, z) = 4.425 (5) Å and O62···C54(x, $y+1$, z) = 3.143 (5) Å. Additional intermolecular C—H(phenyl)···O(carbonyl) weak hydrogen-bond type attractions between neighbouring porphyrin species are also observed (Table 1). Such supramolecular organization is associated with the creation of void space between neighbouring porphyrin molecules. A given node of the open square-grid porphyrin array is a contact point for the methoxycarbonyl groups of four different molecules, which are related to one another by a lattice translation along *a* or *b*. Inversion-related layers pack in a lock-and-key mode, by inserting the axial ligands of one layer into, and partly occupying, half of the interporphyrin voids of a neighbouring layer (Fig. 5). The remaining void space in these layers, and the other half of the interporphyrin voids in every layer, is accommodated in a disordered manner and with partial occupancies by molecules of the pyridine and chloroform solvents. The approximate positions of the solvent moieties are illustrated in Fig. 6. The bilayer domains thus formed also stack in an offset manner in order to optimize van der Waals interactions, by placing the aryl substituents of one bilayer close to the concave porphyrin surfaces of adjacent bilayers (Fig. 5).

The above-described porphyrin supramolecular organization and solvent clathration features are consistent with earlier observations in related tetraarylporphyrin materials, which lack specific hydrogen-bonding or coordination interactions between the porphyrin units [Byrn *et al.*, 1993; Krishna Kumar *et al.*, 1998; CSD, 457 hits (Allen, 2002)].

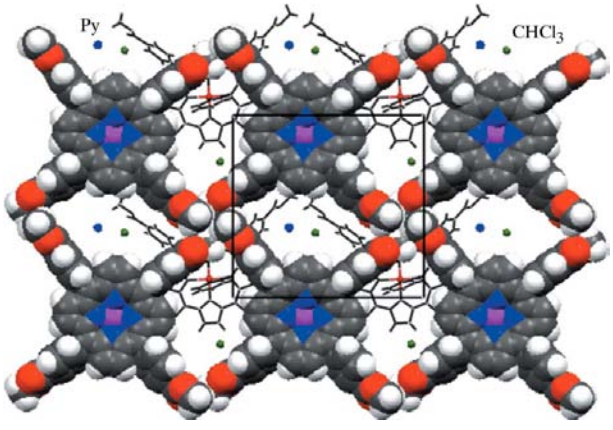

Figure 6
A face-on view of two overlapping layers in (II), in the form of a crystal structure projection down the *c* axis (*a* horizontal and *b* vertical). The upper layer is shown in a space-filling mode, which also illustrates the attractive contacts between the terminal methoxycarbonyl groups of neighbouring porphyrin molecules. The lower porphyrin layer is represented by a stick framework (except for the Zn ions, which are denoted by small spheres). Note that the axial ligands of the lower porphyrin layer penetrate into one set of interporphyrin voids in the upper porphyrin layer. The approximate sites of the solvent molecules in the voids of the upper layer (as derived from the conventional refinement) are represented by discrete spheres; pyridine is represented by the larger spheres and chloroform by the smaller spheres.

Experimental

Compound (I) was synthesized using the Lindsey method (Lindsey *et al.*, 1987) by condensation of pyrrole with 4-(methoxycarbonyl)benzaldehyde. The crude product was purified by silica-gel column chromatography using 2% acetone in chloroform as eluent. Compound (I) was metallated with zinc(II) by reacting (I) (50 mg, 0.06 mmol) with zinc(II) bis(acetate) (133 mg, 0.06 mmol) in methanol (120 ml), affording the metalloporphyrin derivative, zinc-(I). The products were confirmed by ^{1}H NMR and UV–vis (in tetrahydrofuran) spectra. Diffraction-quality crystals of (I) were obtained by dissolving 5 mg (0.006 mmol) of the compound in a minimal amount of chloroform and a few drops of nitrobenzene, followed by slow evaporation over two weeks. Single crystals of (II) were prepared by dissolving zinc-(I) (6 mg, 0.0065 mmol) in a small amount (10 ml) of a chloroform–pyridine mixture (9:1 *v*/*v*) with a few drops of nitrobenzene, followed by slow evaporation in air for 10 d.

Compound (I)

Crystal data

$C_{52}H_{38}N_4O_8\cdot1.904C_6H_5NO_2$
M_r = 1081.27
Monoclinic, $C2/c$
a = 32.6249 (8) Å
b = 7.0657 (2) Å
c = 23.5160 (8) Å
β = 100.2918 (9)°
V = 5333.6 (3) Å^3
Z = 4
D_x = 1.347 Mg m^{-3}
Mo $K\alpha$ radiation
Cell parameters from 5804 reflections
θ = 1.4–28.2°
μ = 0.09 mm^{-1}
T = 110 (2) K
Prism, purple
0.35 × 0.20 × 0.15 mm

Data collection

Nonius KappaCCD area-detector diffractometer
1° φ scans
20139 measured reflections
6404 independent reflections
3904 reflections with $I > 2\sigma(I)$
R_{int} = 0.054
θ_{max} = 28.2°
$h = -41 \rightarrow 42$
$k = -9 \rightarrow 9$
$l = -30 \rightarrow 30$

Refinement

Refinement on F^2	H-atom parameters constrained
$R[F^2 > 2\sigma(F^2)] = 0.057$	$w = 1/[\sigma^2(F_o^2) + (0.0865P)^2]$ where $P = (F_o^2 + 2F_c^2)/3$
$wR(F^2) = 0.158$	$(\Delta/\sigma)_{max} < 0.001$
$S = 1.02$	$\Delta\rho_{max} = 0.30$ e Å^{-3}
6404 reflections	$\Delta\rho_{min} = -0.31$ e Å^{-3}
374 parameters	

Compound (II)

Crystal data

$[Zn(C_{52}H_{36}N_4O_8)(C_5H_5N)]$	Mo $K\alpha$ radiation
$M_r = 989.32$	Cell parameters from 7893 reflections
Orthorhombic, $P2_12_12_1$	$\theta = 1.4$–28.3°
$a = 17.4965$ (4) Å	$\mu = 0.45$ mm^{-1}
$b = 18.2617$ (2) Å	$T = 110$ (2) K
$c = 19.0558$ (4) Å	Prism, purple
$V = 6088.6$ (2) Å^3	0.45 × 0.40 × 0.30 mm
$Z = 4$	
$D_x = 1.079$ Mg m^{-3}	

Data collection

Nonius KappaCCD area-detector diffractometer	$R_{int} = 0.085$
1° φ and ω scans	$\theta_{max} = 28.2^\circ$
52179 measured reflections	$h = -23 \rightarrow 23$
14686 independent reflections	$k = -24 \rightarrow 24$
9268 reflections with $I > 2\sigma(I)$	$l = -25 \rightarrow 25$

Refinement

Refinement on F^2	$w = 1/[\sigma^2(F_o^2) + (0.0727P)^2]$ where $P = (F_o^2 + 2F_c^2)/3$
$R[F^2 > 2\sigma(F^2)] = 0.053$	$(\Delta/\sigma)_{max} = 0.001$
$wR(F^2) = 0.131$	$\Delta\rho_{max} = 0.32$ e Å^{-3}
$S = 0.90$	$\Delta\rho_{min} = -0.40$ e Å^{-3}
14686 reflections	Absolute structure: Flack (1983), with 6502 Friedel pairs
649 parameters	Flack parameter: 0.259 (9)
H-atom parameters constrained	

Table 1
Apparent C—H···O interactions (Å, °).

Compound	Contact	C—H	H···O	C···O	C—H···O
(I)	C2—H2···O43^{i}	0.95	2.45	3.357 (2)	160
(I)	C7—H7···O32^{ii}	0.95	2.30	3.197 (2)	157
(I)	C30—H30···O53^{iii}	0.95	2.51	3.296 (3)	141
(I)	C40—H40···O42^{iv}	0.95	2.43	3.233 (3)	143
(II)	C36—H36···O62^{v}	0.95	2.40	3.293 (4)	147
(II)	C46—H46···O32^{vi}	0.95	2.49	3.418 (4)	164

Symmetry codes: (i) $-x, y, \frac{1}{2} - z$; (ii) $\frac{1}{2} - x, \frac{1}{2} - y, -z$; (iii) $\frac{1}{2} - x, \frac{1}{2} + y, \frac{1}{2} - z$; (iv) $x, 1 + y, z$; (v) $1 - x, y + \frac{1}{2}, \frac{1}{2} - z$; (vi) $\frac{1}{2} + x, \frac{1}{2} - y, -z$.

The H atoms were located in calculated positions and constrained to ride on their parent atoms, with C—H distances in the range 0.95–0.98 Å and with $U_{iso}(H) = 1.2$ or $1.5U_{eq}(C)$. The positional disorder of the pyrrole H atoms in (I) is characterized by occupancy factors of 0.42 (3) and 0.58 (3) for atoms H21 and H22, respectively. Molecules of the nitrobenzene guest occluded in the channels of (I) were refined to have an occupancy of 0.95 at each site. The O63–C64 methoxy group in (II) reveals orientational disorder, which was reasonably well characterized. The relative occupancies are 0.459 (8) for the O63–C64 fragment and 0.541 (8) for the O63′–C64′ fragment. The structure of (II) was then refined as a 1:3 twin. It was found to contain pyridine and chloroform solvent, which could not be modelled reliably. Conventional refinement converged at $R = 0.088$, showing recognisable frameworks of the solvent species with partial occupancies at well defined sites, but with very high anisotropic displacement parameters for the corresponding atoms and with distorted geometries. Correspondingly, it was preferable to subtract the contribution of this solvent from the diffraction data using the SQUEEZE procedure in *PLATON* (Spek, 2003). The modified calculations coverged smoothly at a considerably lower R factor, resulting in a structural model of good precision for the porphyrin lattice, as discussed in this paper. Standard refinement calculations of the entire structure in this case served to locate the guest components in the lattice. The solvent-accessible voids were estimated to be 31% of the crystal volume. The residual electron-density count was assessed as 202 electrons per unit cell, which is consistent with approximately two molecules of pyridine and two molecules of chloroform.

For both compounds, data collection: *COLLECT* (Nonius, 1999); cell refinement: *DENZO* (Otwinowski & Minor, 1997); data reduction: *DENZO*; program(s) used to solve structure: *SIR97* (Altomare *et al.*, 1994); program(s) used to refine structure: *SHELXL97* (Sheldrick, 1997); molecular graphics: *ORTEPIII* (Burnett & Johnson, 1996) and *MERCURY* (Bruno *et al.*, 2002); software used to prepare material for publication: *SHELXL97*.

This research was supported in part by the Israel Science Foundation (grant No. 254/04).

Supplementary data for this paper are available from the IUCr electronic archives (Reference: GD3004). Services for accessing these data are described at the back of the journal.

References

Allen, F. H. (2002). *Acta Cryst.* B**58**, 380–388.
Altomare, A., Cascarano, G., Giacovazzo, C., Guagliardi, A., Burla, M. C., Polidori, G. & Camalli, M. (1994). *J. Appl. Cryst.* **27**, 435.
Bruno, I. J., Cole, J. C., Edgington, P. R., Kessler, M., Macrae, C. F., McCabe, P., Pearson, J. & Taylor, R. (2002). *Acta Cryst.* B**58**, 389–397.
Burnett, M. N. & Johnson, C. K. (1996). *ORTEPIII*. Report ORNL-6895. Oak Ridge National Laboratory, Tennessee, USA.
Byrn, M. P., Curtis, C. J., Hsiou, Y., Khan, S. I., Sawin, P. A., Tendick, S. K., Terzis, A. & Strouse, C. E. (1993). *J. Am. Chem. Soc.* **115**, 9480–9497.
Flack, H. D. (1983). *Acta Cryst.* A**39**, 876–881.
Goldberg, I. (2005). *Chem. Commun.* pp. 1243–1254.
Krishna Kumar, R., Balasubramanian, S. & Goldberg, I. (1998). *Inorg. Chem.* **37**, 541–552.
Lindsey, J. S., Schreiman, I. C., Hsu, H. C., Kearney, P. C. & Marguerettaz, A. M. (1987). *J. Org. Chem.* **52**, 827–836.
Lipstman, S., George, S. & Goldberg, I. (2006). *Acta Cryst.* E**62**, m417–m419.
Lipstman, S. & Goldberg, I. (2006). *Acta Cryst.* E**62**, m158–m160.
Nonius (1999). *COLLECT*. Nonius BV, Delft, The Netherlands.
Otwinowski, Z. & Minor, W. (1997). *Methods in Enzymology*, Vol. 276, *Macromolecular Crystallography*, Part A, edited by C. W. Carter Jr & R. M. Sweet, pp. 307–326. New York: Academic Press.
Sheldrick, G. M. (1997). *SHELXL97*. University of Göttingen, Germany.
Spek, A. L. (2003). *J. Appl. Cryst.* **36**, 7–13.